2012

Single-Phased White-Emitting 12CaO·7Al2O3:Ce3+, Dy3+ Phosphors with Suitable Electrical Conductivity for Field Emission Displays

Xiuling Liu
Northeast Normal University

Yuxue Liu
Northeast Normal University

Duanting Yan
Northeast Normal University

Hancheng Zhu
Northeast Normal University

Chunguang Liu
Northeast Normal University

Recommended Citation

Authors

Xiuling Liu, Yuxue Liu, Duanting Yan, Hancheng Zhu, Chunguang Liu, Changshan Xu, Yichun Liu, and Xiao-Jun Wang

Journal of Materials Chemistry

PAPER

Single-phased white-emitting 12CaO·7Al$_2$O$_3$:Ce^{3+}, Dy^{3+} phosphors with suitable electrical conductivity for field emission displays

Xiuling Liu,[a] Yuxue Liu,*[a] Duanting Yan,[a] Hancheng Zhu,[a] Chunguang Liu,[a] Changshan Xu,[a] Yichun Liu[a] and Xiaojun Wang*[b]

A novel white-light-emitting phosphor, 12CaO·7Al$_2$O$_3$:Ce^{3+}, Dy^{3+} with H$^-$ encaging, was prepared by the solid-state reaction in H$_2$ atmosphere. Upon excitation at 362 nm, the phosphor shows intense white-light emission that combines the blue and yellow emissions at 476 and 576 nm, assigned to the $^4F_{9/2} \rightarrow {}^6H_{15/2}$ and $^4F_{9/2} \rightarrow {}^6H_{13/2}$ transitions of Dy^{3+}, respectively. A weak broad blue emission centered at 430 nm is also observed and attributed to the 5d–4f transitions of Ce^{3+}. The photoluminescence intensity of Dy^{3+} increases greatly with increasing Ce^{3+} concentration, indicating that the effective energy transfer occurred from Ce^{3+} to Dy^{3+} in the phosphor. In particular, the phosphor can be converted to a persistent semiconductor upon ultraviolet irradiation due to the electrons released from the encaged H$^-$ ions, and the electrical conductivity is measured to be 10^{-2} S cm^{-1}. The conductive phosphor exhibits excellent white-light emission (CIE coordinate of (0.324, 0.323)) under low-voltage (5 kV) electron beam excitation, suggesting that the phosphor is a potential candidate for applications in field emission displays.

1. Introduction

Recently, field emission displays (FEDs) have been considered as one of the most promising technologies in flat panel displays because they provide thin panels, self-emission, a distortion-free image, wide viewing angle, low weight, and quick response, as well as low power consumption.[1–4] Phosphors for FEDs are required to have high emission efficiency, good chemical stability, and effective conductivity with high beam current density.[5–8] FED phosphors need to have suitable electrical conductivity because insulating phosphors do not transfer electrons and the charge build-up on the phosphor decreases the efficiency of the phosphor.[9] Although many efficient sulfide-based compounds with suitable electrical conductivity have been explored as possible low voltage phosphors, the volatility of sulfur has prohibited their use in the FEDs.[10–12] Oxide-based phosphors are more stable and environmentally friendly compared to sulfides. However, most oxide-based phosphors have low electrical conductivity. Therefore, it is a challenge to find novel oxide-based phosphors with suitable electrical conductivity and good chemical durability for improving the performance of FED devices.

12CaO·7Al$_2$O$_3$ (C$_{12}$A$_7$) can be an appropriate candidate for such phosphors due to its unique crystal nanocage structure.[13,14]

aCenter for Advanced Optoelectronic Functional Materials Research, Northeast Normal University, 5268 Renmin Street, Changchun 130024, China. E-mail: yxliu@nenu.edu.cn
bDepartment of Physics, Georgia Southern University, Statesboro, GA 30460, USA. E-mail: xwang@GeorgiaSouthern.edu

The unit cell of C$_{12}$A$_7$ consists of 12 cages forming the positively charged [Ca$_{24}$Al$_{28}$O$_{64}$]$^{4+}$ framework and two free O^{2-} occupying randomly two of the 12 cages to maintain the charge neutrality. Hosono *et al.* have converted C$_{12}$A$_7$ from an insulator into a semiconductor by doping with H$^-$ ions followed by irradiation with ultraviolet (UV) light and investigated its electrical properties.[13] The oxygen ions can also be replaced by electrons through reduction treatment[15,16] to form C$_{12}$A$_7$:e$^-$, a new type of electride that can be applied as an excellent field electron emitter in FED devices due to its low work function and stability at room temperature.[17] We have prepared C$_{12}$A$_7$:Er^{3+} and C$_{12}$A$_7$:Tb^{3+} phosphors with intense green emissions and C$_{12}$A$_7$:Dy^{3+} phosphor with the yellowish white emission.[18–20] As a result, C$_{12}$A$_7$ doped with rare earth and H$^-$ ions followed by irradiation with UV light can serve as a phosphor for FEDs with dual functions in both luminescence and conductivity. The same matrix materials can be used as both anode phosphor and cathode electron field emitter for FEDs.

Moreover, single-phased white-light-emitting phosphors are needed for making white-light sources for applications such as solid-state multicolor three-dimensional display and back light, which have led to very active research efforts in the phosphor synthesis.[21,22] However, little research work has been done in dealing with single-phased phosphors with white cathodoluminescence (CL) suitable for applications as backlights in FEDs.[11,23]

In this paper, we prepared C$_{12}$A$_7$:Ce^{3+}, Dy^{3+} as single-phased white-light-emitting phosphors by solid-state reactions. Their photoluminescence (PL), CL, and electrical conductivity have

This journal is © The Royal Society of Chemistry 2012

J. Mater. Chem., 2012, **22**, 16839–16843 | 16839

been investigated in detail. The phosphor shows excellent white-light emission (CIE coordinate of (0.324, 0.323)) under low-voltage electron beam excitation and the electrical conductivity is measured to be a high value of 10^{-2} S cm^{-1}. The new $C_{12}A_7$:Ce^{3+}, Dy^{3+} phosphor system overcomes the disadvantages mentioned above and our results indicate that it has a great potential for applications in FED devices.

2. Experimental

$C_{12}A_7$:x% Ce^{3+}, y% Dy^{3+} powders were synthesized by solid-state reactions using CaCO$_3$ (99.99%), Al$_2$O$_3$ (99.99%), CeO$_2$ (99.99%), and Dy$_2$O$_3$ (99.99%) as the starting materials. The ingredients were quantitatively mixed, and then pre-fired at 850 °C in air atmosphere for 2 hours. After cooling down to room temperature, the pre-fired samples were thoroughly reground and subsequently calcined at 1350 °C in a reducing atmosphere of 20% H$_2$/80% N$_2$ (the flow rate of the gas was 40 ml min^{-1}) for 8 hours to introduce H$^-$ ($C_{12}A_7$:H$^-$).[13] The dense polycrystalline $C_{12}A_7$:H$^-$, Ce^{3+}, Dy^{3+} pellet was fabricated for Hall electrical measurement.

The X-ray diffraction (XRD) patterns were performed on a Rigaku D/max-RA X-ray diffraction spectrometer using Cu Kα radiation (the line of 0.15418 nm). The morphology was characterized by scanning electron microscopy (SEM, FEI, Quanta FEG 250). Diffuse reflectance spectra were taken using a Lambda 900 UV/VIS/NIR spectrophotometer (Perkin Elmer, USA). The PL measurement was recorded using a SHIMADZU RF-5301PC spectrofluorometer. The CL measurement was performed using a MonoCL4 system (Gatan UK) attached to an SEM, in which the phosphors were excited by an electron beam (accelerating voltage = 5 kV, filament current = 270 μA). The electrical property was investigated by a Hall effect electrical measurement system (Lakeshore, 7704) in the van der Pauw configuration. All measurements were performed at room temperature.

3. Results and discussion

The XRD patterns of $C_{12}A_7$:x% Ce^{3+}, y% Dy^{3+} are presented in Fig. 1 (x = 0.1, 0.2, 1.0 and y = 0.1). The main diffraction peaks are in good agreement with the standard powder diffraction data
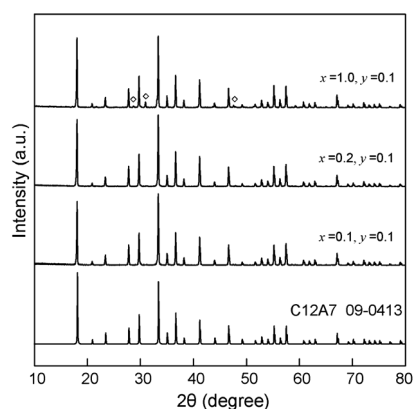
($C_{12}A_7$, JCPDS: 09-0413). Ce^{3+} has an ionic radius of 1.03 Å and Dy^{3+} 0.91 Å, both of which are much larger than that of Al^{3+} (0.39 Å, CN = 4). Therefore, it is reasonable to suggest that Ce^{3+} and Dy^{3+} ions preferentially substitute for Ca^{2+} ions with an equivalent radius (0.99 Å) in $C_{12}A_7$. When $x \geq 1$, an unknown phase will appear as depicted in Fig. 1. When $y > 0.1$, some additional phase similar to CaDyAlO$_4$ is also found in $C_{12}A_7$. The concentration of Dy^{3+} ion is fixed at 0.1% in order to gain strong luminescence and avoid phase change.

Fig. 2 shows the singly doped emission ($C_{12}A_7$:1.0% Ce^{3+}, Fig. 2a, dashed line) and excitation ($C_{12}A_7$:0.1% Dy^{3+}, Fig. 2a, solid line) spectra and the excitation spectrum for a co-doped sample ($C_{12}A_7$:1.0% Ce^{3+}, 0.1% Dy^{3+}, Fig. 2b). The singly doped $C_{12}A_7$:1.0% Ce^{3+} possesses a broad band emission centered at 430 nm, which is attributed to the transitions from 5d^1 to $^2F_{5/2}$ and $^2F_{7/2}$. The excitation spectrum of singly doped $C_{12}A_7$:0.1% Dy^{3+} yields abundant absorption bands in the 300–480 nm range, attributed to the f–f transitions from the ground state $^6H_{15/2}$ to the various excited states of the Dy^{3+} ions. A significant spectral overlap is observed between the emission band of $C_{12}A_7$:1.0% Ce^{3+} and the excitation band of $C_{12}A_7$:0.1% Dy^{3+}, making it possible to have an efficient energy transfer from Ce^{3+} to Dy^{3+}. The excitation spectrum of the co-doped $C_{12}A_7$:1.0% Ce^{3+}, 0.1% Dy^{3+} strongly supports the occurrence of the energy transfer, as shown in Fig. 2b.[24] The f–d absorption bands of Ce^{3+} in the near UV region dominate the excitation spectrum while emission of Dy^{3+} at 576 nm ($^4F_{9/2} \rightarrow ^6H_{13/2}$) is monitored. The excitation band centred at 455 nm ($^6H_{15/2} \rightarrow ^4I_{15/2}$) is most effective in the singly doped $C_{12}A_7$:0.1% Dy^{3+}, but in the co-doped $C_{12}A_7$:1.0% Ce^{3+}, 0.1% Dy^{3+} sample, the intensity of the dominating excitation band (peaked at 362 nm) due to Ce^{3+} is about 140 times stronger than that of the $^6H_{15/2} \rightarrow ^4I_{15/2}$ transition of Dy^{3+}. The efficient energy transfer allows us to take advantage of the strong 4f–5d absorption in Ce^{3+} and to improve the PL efficiency of Dy^{3+}.

Fig. 3 exhibits the emission of $C_{12}A_7$:x% Ce^{3+}, 0.1% Dy^{3+}. When excited at 362 nm, which is in the efficient excitation region of Ce^{3+}, $C_{12}A_7$:x% Ce^{3+}, 0.1% Dy^{3+}, bluish white emission of the

Fig. 1 XRD patterns of $C_{12}A_7$:x% Ce^{3+}, 0.1% Dy^{3+}. (◇ represents the unknown phase).
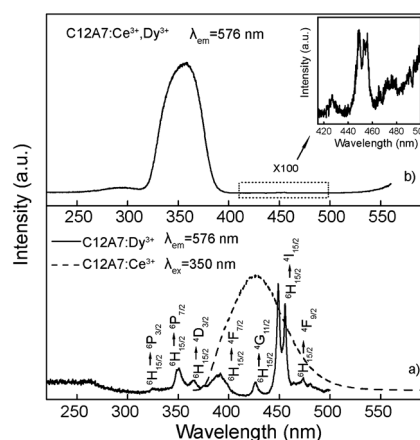
Fig. 2 (a) Emission spectrum of $C_{12}A_7$:1.0% Ce^{3+} (dashed line) and excitation spectrum of $C_{12}A_7$:0.1% Dy^{3+} (solid line). (b) Excitation spectrum of $C_{12}A_7$:1.0% Ce^{3+}, 0.1% Dy^{3+}. The inset shows an enlarged view in the 420–500 nm range.

16840 | *J. Mater. Chem.*, 2012, **22**, 16839–16843

This journal is © The Royal Society of Chemistry 2012

phosphors can be seen through naked eyes. The broad band centred at 430 nm is due to the Ce^{3+} emission, as observed in Fig. 2. The narrow bands centered at 476 and 576 nm are assigned to the $^4F_{9/2} \rightarrow {}^6H_{15/2}$ and $^4F_{9/2} \rightarrow {}^6H_{13/2}$ transitions of Dy^{3+}, respectively. With increasing Ce^{3+} concentration, the PL intensity of Dy^{3+} is found to increase greatly, as revealed in Fig. 3. The luminescence intensity of $C_{12}A_7$:1.0% Ce^{3+}, 0.1% Dy^{3+} sample can be enhanced by 20 times compared to $C_{12}A_7$:0.1% Dy^{3+}, as shown in the inset of Fig. 3. The above results further suggest that more effective energy transfer occurred from Ce^{3+} to Dy^{3+} in $C_{12}A_7$:1% Ce^{3+}, 0.1% Dy^{3+} samples.

To obtain conductive phosphors, $C_{12}A_7$:1.0% Ce^{3+}, 0.1% Dy^{3+} powder and pellet samples were adequately irradiated with UV light (302 nm, 20 W). The colour of the samples changes from white to dark green and a new optical absorption band centred at 2.78 eV appears, as shown in Fig. 4. The irradiation was stopped when the colour of the samples became stable. The phenomena are consistent with that reported by Hosono et al.,[13] who have attributed this absorption band to an F^+-like centre created by trapping an electron in the cage and proved that the UV irradiation caused electron release from the encaged H^- ions, as expressed by the following reaction:[25]

$$H^-(c) + O^{2-}(c) + null(c) \rightarrow OH^-(c) + 2e^-(c), \quad (1)$$
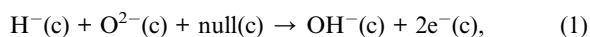
where c and null denote the species in a cage and an empty cage, respectively. Sushko et al.[26] further considered that $C_{12}A_7$:H^- is most sensitive to a wavelength around 300 nm (~4.1 eV), which corresponds to a charge-transfer transition from the encaged H^- state to the cage conduction band (CCB) state localized in the neighbouring cage, as shown in the inset of Fig. 4. These encaged electrons could move over subnanosized cages of the $C_{12}A_7$ lattice via polaron hopping and convert the insulating $C_{12}A_7$ into a persistent electronic conductor.[26] It is believed that electrons are successfully incorporated into $C_{12}A_7$:1.0% Ce^{3+}, 0.1% Dy^{3+} phosphors after irradiating with UV light.

Furthermore, an empirical relation can be established between the absorption peak position, E_{sp}, and the electron concentration, N_e:[27]
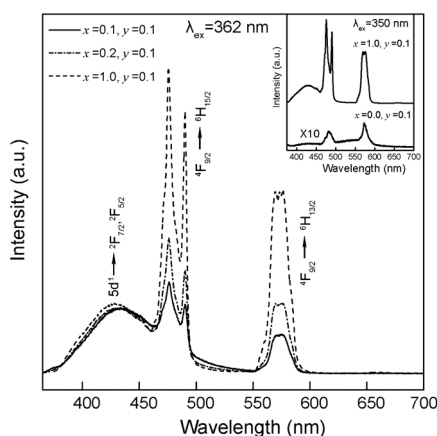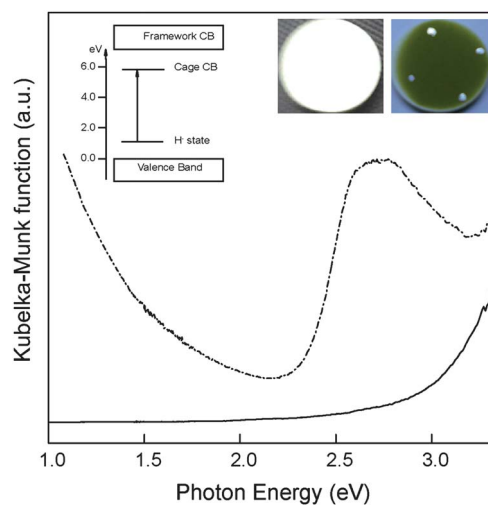
Fig. 4 The absorption spectra of $C_{12}A_7$:1.0% Ce^{3+}, 0.1% Dy^{3+} before (solid line) and after (dash-dotted line) UV irradiation. The insets are photos of $C_{12}A_7$:1.0% Ce^{3+}, 0.1% Dy^{3+} pellets before (left) and after (right) UV irradiation.

$$N_e = [-(E_{sp} - E_{sp}^0)/0.119]^{0.782}, \quad (2)$$

where the low-N_e limit $E_{sp}^0 = 2.83$ eV at $N_e \approx 1 \times 10^{18}$ cm^{-3}. The N_e value of $C_{12}A_7$:1.0% Ce^{3+}, 0.1% Dy^{3+} phosphor evaluated from the above relation is ~10^{20} cm^{-3}. This value is slightly higher than the electron concentration of pure single crystal $C_{12}A_7$ (2×10^{19} cm^{-3}),[13] which may be attributed to our polycrystalline sample with a higher specific surface area and the doped trivalent rare earth ions. The higher specific surface area might be beneficial for more encaged H^- formation during the annealing process. On the other hand, the charge compensation due to the substitution of trivalent Ce^{3+} and Dy^{3+} ions for divalent Ca^{2+} ions might induce more free O^{2-} ions in $C_{12}A_7$:Ce^{3+}, Dy^{3+}. Based on eqn (1), more encaged H^- and O^{2-} will create more encaged electrons after UV irradiation. Furthermore, the electrical conductivity of the irradiated high-density polycrystalline $C_{12}A_7$:1.0% Ce^{3+}, 0.1% Dy^{3+} pellet is measured at a value of 10^{-2} S cm^{-1}, which is far higher than that of Y_2O_3:Eu^{3+} phosphors coated with In_2O_3 (5.2 μS cm^{-1}).[28] The results indicate that $C_{12}A_7$:1.0% Ce^{3+}, 0.1% Dy^{3+} system with encaged electrons has an advantage with regard to FED devices compared with other insulating oxide-based phosphors.

In addition, the SEM image of the irradiated $C_{12}A_7$:1.0% Ce^{3+}, 0.1% Dy^{3+} powders without gold-plating was obtained, as represented in Fig. 5. The clear image indicates that there is no charge build-up. The slightly aggregated particles have an approximately spherical shape and a narrow size range of 1.5–2.5 μm, which is perfect to produce a compact phosphor screen and thus to improve its CL property.[29]

It is interesting to note that the intensity ratio of yellow to blue (Y/B) emissions of Dy^{3+} increases substantially and the overall luminescence intensity declines slightly after UV irradiation, as plotted in Fig. 6. It is known that the yellow emission ($^4F_{9/2} \rightarrow {}^6H_{13/2}$) belongs to the hypersensitive transition (forced electric dipole), and its intensity is strongly influenced by the environment around the Dy^{3+} ions. The encaged anions in $C_{12}A_7$ can induce a considerable deformation of its lattice, which can be

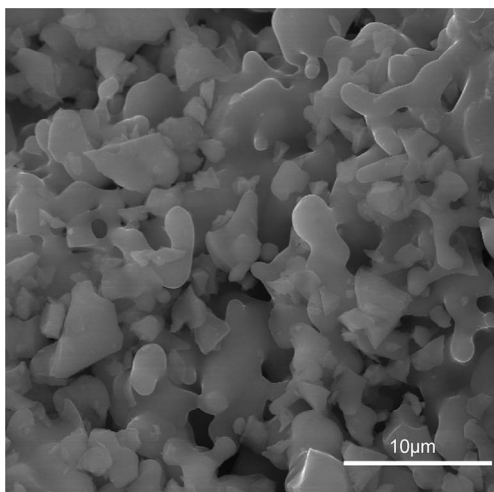**Fig. 3** Emission spectra of $C_{12}A_7$:x% Ce^{3+}, 0.1% Dy^{3+}. The inset shows emission spectra of $C_{12}A_7$:0.1% Dy^{3+} and $C_{12}A_7$:1.0% Ce^{3+}, 0.1% Dy^{3+} under 350 nm excitation.

Fig. 5   SEM image of $C_{12}A_7$:1.0% Ce^{3+}, 0.1% Dy^{3+}.

Fig. 7   The CL spectra of $C_{12}A_7$:1.0% Ce^{3+}, 0.1% Dy^{3+} (solid line) and $C_{12}A_7$:0.1% Dy^{3+} (dashed line).

measured by the Ca–Ca distance in the cage, $D_{Ca–Ca}$, where the two Ca ions occupy the sites on the opposite sides of the cage.[16] $D_{Ca–Ca}$ (5.63 Å) of the electron-encaging cage is much larger than that of H^- and OH^- (4.9 Å), O^{2-} (4.27 Å) encaging cages, and more close to that of the empty cage (5.77 Å). The larger the deformation induced, the lower the symmetry of the lattice framework created. As a result, the high symmetry of the crystal field will be resumed after H^- ions release electrons under UV irradiation. The change of symmetry may be responsible for the decrease of the overall luminescence intensity with more decrease in the blue region in comparison with the yellow emission. The blue emission was absorbed by F^+-like centres while the yellow is transparent in the sample (the absorption band peaked at 2.78 eV, as shown in Fig. 4). As a consequence, the intensity ratio of Y/B emissions of Dy^{3+} increases after the UV irradiation.

Fig. 7 displays the CL spectra of the UV irradiated $C_{12}A_7$:0.1% Dy^{3+} and $C_{12}A_7$:1.0% Ce^{3+}, 0.1% Dy^{3+} phosphors under low-voltage (5 kV) electron beam excitation. The CL spectra are very similar to the PL emissions (Fig. 3 or 6) and the luminescence intensity of the co-doped sample is stronger than that of the singly doped sample by a factor of 2 to 3, suggesting that the energy transfer from Ce^{3+} still enhances the Dy^{3+} emission under
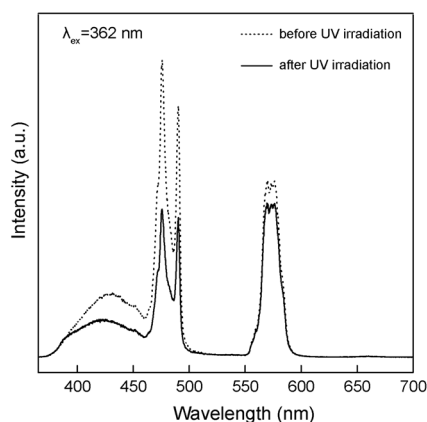

Fig. 8   The CIE chromaticity diagram for $C_{12}A_7$:1.0% Ce^{3+}, 0.1% Dy^{3+} and $C_{12}A_7$:0.1% Dy^{3+} under low-voltage electron beam excitation.

the electron beam excitation. The energy transfer is less efficient in comparison with PL because the excitation energy distribution of the secondary electrons created by the CL source is very broad. Absorption is not dominated by Ce^{3+} as performed in PL upon a single wavelength excitation at 362 nm, but occurs at all the excited states of Ce^{3+} and Dy^{3+} in CL. Meanwhile, the CIE coordinate of $C_{12}A_7$:1.0% Ce^{3+}, 0.1% Dy^{3+} (0.324, 0.323) is closer to the standard white light (0.33, 0.33) than $C_{12}A_7$:0.1% Dy^{3+} (0.355, 0.364) and LaOCl:Tb^{3+}, Sm^{3+} (0.3405, 0.3207),[23] as shown in Fig. 8.

4.   Conclusions

In summary, $C_{12}A_7$:Ce^{3+}, Dy^{3+} has been prepared by the solid-state reaction as a single-phased, white-light emission phosphor. Co-doping of Ce^{3+} has enhanced the PL intensity of Dy^{3+} significantly due to the effective energy transfer from Ce^{3+} to Dy^{3+}. The phosphor can be transformed from an insulator to a semiconductor by UV irradiation and exhibits an excellent white light emission under low-voltage electron beam excitation. The new phosphor has advantages such as chemical stability, electrical conductivity, CIE chromaticity, low-cost preparation, and

Fig. 6   Emission spectra of $C_{12}A_7$:1.0% Ce^{3+}, 0.1% Dy^{3+} before (dashed line) and after (solid line) UV irradiation.

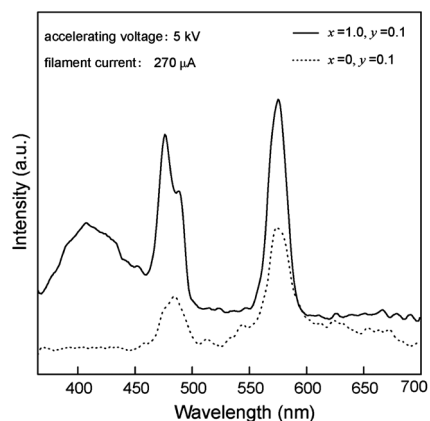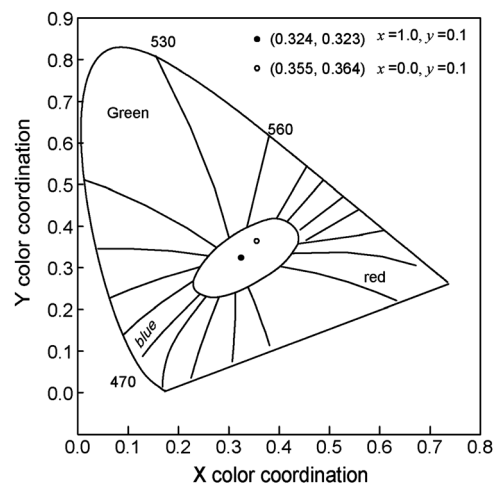environmentally friendly nature, making it a great candidate for applications in FED devices.

Acknowledgements

References

1 T. Jüstel, H. Nikol and C. Ronda, *Angew. Chem., Int. Ed.*, 1998, **37**, 3084.
2 S. Itoh, M. Tanaka and T. Tonegawa, *J. Vac. Sci. Technol., B*, 2004, **22**, 1362.
3 G. Li, X. Zhang, C. Peng, M. Shang, D. Geng, Z. Cheng and J. Lin, *J. Mater. Chem.*, 2011, **21**, 6477.
4 G. Li, Z. Hou, C. Peng, W. Wang, Z. Cheng, C. Li, H. Lian and J. Lin, *Adv. Funct. Mater.*, 2010, **20**, 3446.
5 M. Leskelä, *J. Alloys Compd.*, 1998, **275–277**, 702.
6 S. Shionoya, W. M. Yen and H. Yamamoto, *Phosphor Handbook*, CRC Press, Boca Raton, 2006, pp. 545–546.
7 X. Liu and J. Lin, *J. Mater. Chem.*, 2008, **18**, 221.
8 X. Liu and J. Lin, *Appl. Phys. Lett.*, 2007, **90**, 184108.
9 I. Yu, *Mater. Res. Bull.*, 2006, **41**, 1403.
10 F. L. Zhang, S. Yang, C. Stoffers, J. Penczek, P. N. Yocom, D. Zaremba, B. K. Wagner and C. J. Summers, *Appl. Phys. Lett.*, 1998, **72**, 2226.
11 Y. C. Li, Y. H. Chang, Y. F. Lin, Y. J. Lin and Y. S. Chang, *Appl. Phys. Lett.*, 2006, **89**, 081110.
12 M. Shang, G. Li, D. Yang, X. Kang, C. Zhang and J. Lin, *J. Electrochem. Soc.*, 2011, **158**, 125.
13 K. Hayashi, S. Matsuishi, T. Kamiya, M. Hirano and H. Hosono, *Nature*, 2002, **419**, 462.
14 S. Matsuishi, Y. Toda, M. Miyakawa, K. Hayashi, T. Kamiya, M. Hirano, I. Tanaka and H. Hosono, *Science*, 2003, **301**, 626.
15 K. Hayashi, P. V. Sushko, A. L. Shluger, M. Hirano and H. Hosono, *J. Phys. Chem. B*, 2005, **109**, 23836.
16 S. W. Kim, S. Matsuishi, T. Nomura and Y. Kubota, *Nano Lett.*, 2007, **7**, 1138.
17 Y. Toda, S. Matsuishi, K. Hayashi, K. Ueda, T. Kamiya, M. Hirano and H. Hosono, *Adv. Mater.*, 2004, **16**, 685.
18 D. Wang, Y. X. Liu, Y. C. Liu, C. S. Xu, C. L. Shao and X. H. Li, *J. Nanosci. Nanotechnol.*, 2008, **8**, 1458.
19 L. L. Xue, Y. X. Liu, C. S. Xu, Y. C. Liu, C. J. Zhao and X. T. Zhang, *J. Nanosci. Nanotechnol.*, 2010, **10**, 2125.
20 H. C. Zhu, Y. X. Liu, D. T. Yan and X. L. Yan, *J. Nanosci. Nanotechnol.*, 2011, **11**, 9958.
21 J. S. Kim, P. E. Jeonny, J. C. Choi, H. L. Park, S. I. Mho and G. C. Kim, *Appl. Phys. Lett.*, 2004, **84**, 2931.
22 G. Li, C. Li, C. Zhang, Z. Cheng, Z. Quan, C. Peng and J. Lin, *J. Mater. Chem.*, 2009, **19**, 8936.
23 G. Li, C. Li, Z. Hou, C. Peng, Z. Cheng and J. Lin, *Opt. Lett.*, 2009, **34**, 3833.
24 J. Lin and Q. Su, *J. Mater. Chem.*, 1995, **5**, 1151.
25 K. Hayashi, *J. Phys. Chem. C*, 2011, **115**, 11003.
26 P. V. Sushko, A. L. Shluger, K. Hayashi, M. Hirano and H. Hosono, *Appl. Phys. Lett.*, 2005, **86**, 1.
27 S. Matsuishi, T. Nomura, M. Hirano, K. Kodama, S. I. Shamoto and H. Hosono, *Chem. Mater.*, 2009, **21**, 2589.
28 M. Zhang, X. Wang, H. Ding, H. Li, L. Pan and Z. Sun, *Int. J. Appl. Ceram. Technol.*, 2011, **8**, 752.
29 G. Li, X. Xu, C. Peng, M. Shang, D. Geng, Z. Cheng, J. Chen and J. Lin, *Opt. Express*, 2011, **19**, 16423.

This journal is © The Royal Society of Chemistry 2012

J. Mater. Chem., 2012, **22**, 16839–16843 | 16843